Supplementary Methods

Histopathologic Analysis

Jejunum tissues from mice were fixed in either 10 % formalin or 4 % paraformaldehyde, embedded in paraffin or OCT, respectively, and cut into 5 μm sections. Immunohistochemistry was performed as described previously[1]. In situ hybridization was performed as described previously[2], or using the RNAscope kit.

Antibodies for immunohistochemistry

The primary antibodies used included the following: Ki67 (1:200, Abcam), β-catenin (1:500, BD laboratories), BrdU (1:500, Dako), GFP (1:400, Invitrogen), RFP (1:400, Rockland), chromogranin A (1:500, Abcam), DCLK1 (1:500, Abcam), FABP1 (1:500, R&D), MUC2 (1:500, Santa Cruz), Lysozyme (1:1000, Dako), Synaptophysin (1:200, Abcam), HES1 (1:100, Cell Signaling), TAC1 (1:100, Abcam), cyclin D1 (1:200, Abcam), SOX9 (1:200, Santa cruz), KRT7 (1:1000, Serotec), CDX2 (1:200, Abcam), Lysozyme (1:1000, Dako), estrogen receptor alpha (Abcam), carbonic anhydrase 2 (1:500, Sino biological), YAP (1:200, Cell Signaling), UEA-I (1:1000, Vector), Bhlha15 (1:200, Cell Signaling), cleaved caspase 3 (1:200, Cell Signaling), and DLL1 (1:200, R&D). For secondary

antibodies, biotinylated secondary antibodies (Vectastain ABC kit; Vector Laboratories) and Alexa fluor 488 or 594 or 647 secondary antibodies (Invitrogen) were used. For staining of human samples, colon disease tissue array and small intestine tissue array (US Biomax) was used. For EdU and TUNEL detection, Click-IT Alexa fluor 488 imaging kits (Invitrogen) were used.

Quantitative RT-PCR (qRT-PCR)

Total RNA was extracted from whole jejunum samples or sorted cells using TRIzol reagent (Invitrogen) or the RNAqueous-micro kit (Ambion) and subjected to first-strand complementary DNA synthesis using the Superscript III cDNA Amplification System (Invitrogen). qRT-PCR was performed an ABI 7300 system and SYBR green (Roche). The results were expressed as the copy number of each gene relative to that of *B2m*.

Microarray analysis

RNAs from sorted cells were applied to GeneChip 3'IVT Pico Reagent Kit (Affymetrix). Data was analyzed on the $\log_2$ scale using Subio platform (Subio inc. Japan). The significance of differential expression of microarray data was analyzed using the empirical Bayesian method. Transcripts with Benjamini-Hochberg false discovery rates less than 0.05 as well as more than

2-fold upregulation and less than 0.5-fold downregulation were considered to be differentially expressed. GSEA analysis was performed as described previously[3, 4]. Significance (p value) and false discovery rate (FDR, q value) of the enrichment scores were determined using 1,000 permutations of random gene sets of similar size. Similarly, 500 transcripts with the highest enrichment in ISCs, enterocyte progenitors, *Dll1*$^{+}$ progenitors, and label rataining cells compared to Paneth cell population were determined by using previously published datasets[4-7], and analyzed to examine the specificity for indicated populations.

Gland isolation, in vitro culture, and FACS

The harvested mouse jejunums were opened longitudinally and washed with cold PBS. Villus compartment was removed by a razor edge, the tissue was chopped into approximately 5 mm pieces, washed with cold PBS, and incubated in 2 mM EDTA in PBS for 60 min on ice. The tissue fragments were suspended vigorously in cold 10 % FBS using a 10-mL pipette, yielding supernatants enriched in crypts. Gland fractions were centrifuged at 900 rpm for 6 min at 4 ℃ and diluted with advanced DMEM/F12 (Invitrogen) containing B27, N2, 1 μM n-Acetylcysteine, 10 mM HEPES, penicillin/streptomycin, and Glutamax (all from Invitrogen). Samples were passed through 100-μm filters (BD Biosciences) and

centrifuged at 720 rpm for 5 min at 4℃, and single cells were discarded. Isolated crypts were embedded in Matrigel (Corning) and 500 crypts/well were seeded in a pre-warmed 24-well plate. After the Matrigel solidified, it was overlaid with advanced DMEM/F12 medium containing 50 ng/mL EGF (Invitrogen), 100 ng/mL Noggin (Peprotech), and 1 μg/mL R-spondin 1. In some experiments, 10 μg/mL Wnt3a or 1μM Jagged-1 was added. All medium contents were changed three times a week. Single cells were isolated and cultured as described previously[8]. Glands were dissociated using TrypLE express (Invitrogen) including 1 mg/mL DNase I (Roche) for 10 min at 37 ℃. Dissociated ce lls were passed through a 20-μm cell strainer and washed with 2 % FBS/PBS. Viable epithelial single cells were gated by forward scatter, side scatter and a pulse-width parameter, and propidium iodide-negative staining. For staining, cell suspensions were incubated with conjugated monoclonal antibodies against CD24 (Biolegend). For quantification of cell proportion and RT-PCR, 3 biological replicates were used. For single cell culture analysis, cells were sorted and collected from 3 mice/group, then pelleted and 1000 singlet cells per well were embedded in extracellular matrix and cultured (3 wells/group). Experiments were repeated in 2 independent cohorts and representative data were shown.

Analysis of TCGA dataset.

TCGA dataset was analyzed by using cBioPortal (http://www.cbioportal.org/). Tumor histology was obtained from Cancer Digital Slide Archive (http://cancer.digitalslidearchive.net/). Serrated features were defined by the presense of complex villiform structure with characteristic serration by professional pathologists.

Statistical Analysis

The differences between the means were compared using either the Student's *t*-test or the Wilcoxon test. $p < 0.05$ was considered to indicate statistical significance. In Tables, we used Fisher's test and chi-square test.

References

1. Hayakawa Y, Jin G, Wang H, et al. CCK2R identifies and regulates gastric antral stem cell states and carcinogenesis. Gut 2015;64:544-53.
2. Sakitani K, Hayakawa Y, Deng H, et al. CXCR4-expressing Mist1(+) progenitors in the gastric antrum contribute to gastric cancer development. Oncotarget 2017;8:111012-111025.
3. Stange DE, Koo BK, Huch M, et al. Differentiated troy(+) chief cells act as reserve stem cells to generate all lineages of the stomach epithelium. Cell 2013;155:357-68.
4. Jadhav U, Saxena M, O'Neill NK, et al. Dynamic Reorganization of Chromatin Accessibility Signatures during Dedifferentiation of Secretory Precursors into Lgr5+ Intestinal Stem Cells. Cell Stem Cell 2017;21:65-77 e5.
5. van Es JH, Sato T, van de Wetering M, et al. Dll1+ secretory progenitor cells revert to stem cells upon crypt damage. Nat Cell Biol 2012;14:1099-104.
6. Roth S, Franken P, Sacchetti A, et al. Paneth cells in intestinal homeostasis and tissue injury. PLoS One 2012;7:e38965.

7. Merlos-Suarez A, Barriga FM, Jung P, et al. The intestinal stem cell signature identifies colorectal cancer stem cells and predicts disease relapse. Cell Stem Cell 2011;8:511-24.
8. Sato T, Vries RG, Snippert HJ, et al. Single Lgr5 stem cells build crypt-villus structures in vitro without a mesenchymal niche. Nature 2009;459:262-5.

Table S1. Association between Notch-related gene alteration, molecular subtype, primary tumor site, and histological serrated feature (N=194).

	Notch-related gene alteration N=86, (%)	No Notch-related alteration N=108, (%)	P value
Molecular subtype			
CIN	54 (62.79)	26 (24.07)	**<0.001**
Invasive	15 (17.44)	38 (35.19)	0.244
MSI/CIMP	17 (19.77)	44 (40.74)	**0.010**
Primary tumor site*			
Right	17 (20.00)	39 (36.11)	**0.030**
Transverse	4 (4.71)	7 (6.48)	0.082
Left	45 (52.94)	20 (18.52)	0.084
Rectum	19 (22.35)	42 (38.89)	0.191
Serrated feature**	37 (43.53)	23 (21.50)	**0.001**

*Missing data included (n=1).

**Missing data included (n=2).

Table S2. Association between tumors with serrated features and genetic mutations (N=192)

	With serrated features N=60, (%)	Without features N=132, (%)	P value
Notch alterations	37 (61.67)	48 (36.36)	**0.001**
APC mutations	49 (81.67)	98 (74.24)	0.260
KRAS mutations	31 (51.67)	49 (37.12)	0.058
BRAF mutations	5 (8.33)	3 (2.27)	0.051
TP53 mutations	31 (51.67)	69 (52.27)	0.938

Supplementary figure legends

Figure S1. Bhlha15, Lgr5, and CD24 expression in the small intestine.

(A) (Left) Staining for estrogen receptor (red) in *Bhlha15*-CreERT mouse intestine that can visualize CreERT. Negative control image using WT mice is provided. (Middle) Staining for estrogen receptor (green) and UEA-I (red) in *Bhlha15*-CreERT mouse intestine. (Right) *Bhlha15* in situ hybridization and Bhlha15 staining of in small intestinal crypt. Yellow arrows indicate $CreERT^+$ Paneth cells; red arrows indicate $CreERT^+$ TA cells. (B) (Top) $TdTomato^+$ cell distribution in small intestinal villus-crypt units in *Bhlha15*-CreERT; *R26*-TdTomato mice at indicated time points. Numbers of $TdTomato^+$ regions (crypts, L; lower villus, M; upper villus, U) per 100 recombined units were quantified. (Middle) Average numbers of $TdTomato^+$ cells in villus-crypt units in *Bhlha15*-CreERT; *R26*-TdTomato mice at indicated time points. Mean±S.E.M. Total 50 units from 2 mice at each time point were quantified. (Bottom) Proportion of cell types in $TdTomato^+$ cells at each time point. Paneth cells are defined by Lysozyme staining; enteroendocrine cells by chromogranin A; tuft cells by DCLK1; goblet cells by MUC2; TA cells by negative staining for these markers and cell position. Total 300 $TdTomato^+$ cells from 2 mice are analyzed at

each time point. (C) GFP (green) and estrogen receptor (red) staining on *Bhlha15*-CreERT; *Lgr5*-DTR-GFP mouse intestine. S, secretory precursors; P, Paneth cells; C, CBCs. Arrows indicate double positive cells. (D) Protocol for label retention assay (top) and representative images (bottom) of EdU detection (green) with RFP staining (red). EdU was given to *Bhlha15*-CreERT; *R26*-TdTomato mice intraperitoneally for 3 times in every 12 hours, then drinking water is given for 10 days. Tamoxifen was given 1 day prior to sacrifice. Doxorubicin was given once during EdU pulse in doxorubicin (+) group. (E) Percentage of TdTomato$^+$ cells in EdU$^+$ cells. Total 120 EdU$^+$ cells from 2 mice per group were quantified. (F-G) FACS plots and histograms of CD24-stained TdTomato$^+$ and GFP$^+$ cells isolated from *Bhlha15*-CreERT; *Lgr5*-DTR-GFP; *R26*-TdTomato mice. Negative control sample which was stained with control IgG antibody is shown at the bottom.

Figure S2. Relationship between Bhlha15 and DLL1 expression in the small intestine.

(A) Staining for DLL1 (green) and estrogen receptor (red, left), and Bhlha15 (red, right) in *Bhlha15*-CreERT mice. Green arrows indicate DLL1$^+$ cells; red arrows indicate CreERT$^+$ or Bhlha15$^+$ TA cells. (B) Percentage of DLL1$^+$ and DLL1$^-$ cells

in TdTomato^{+} cells in *Bhlha15*-CreERT; *R26*-TdTomato mice 1 day after tamoxifen (left) and Percentage of DLL1^{+} and DLL1^{-} cells in CreERT^{+} cells in *Bhlha15*-CreERT mice. Total 300 cells from 3 mice per group are counted. (C) Double in situ hybridization for *Bhlha15* (blue) and *Dll1* (pink). Representative images from crypt and villus compartments are shown. Pink arrows indicate *Dll1*$^{+}$ cells; blue arrows indicate *Bhlha15*$^{+}$ cells; purple arrow indicates rare goblet cells that contain a few *Bhlha15* and *Dll1* transcripts in villus. (D) Percentage of Ki67^{+} cells in Tomato^{+} Paneth cells and non-Paneth TA cells in *Bhlha15*-CreERT; *R26*-TdTomato mice 1 day after tamoxifen. Total 300 TdTomato^{+} cells per group were counted. n=3/group. (E) Percentage of Ki67^{+} cells in TdTomato^{+} cells in TA zone (not including Paneth cells) at each time point. (F) Ki67 (green), RFP (red), and MUC2 (gray) staining on *Bhlha15*-CreERT; *R26*-TdTomato mice 2 days after tamoxifen. Red arrows indicate MUC2^{+}TdTomato^{+}Ki67^{-} mature goblet cells; yellow arrow indicates MUC2^{-}TdTomato^{+}Ki67^{+} immature progenitor cells; green arrow indicates MUC2^{+}TdTomato^{+}Ki67^{+} pre-goblet cells. Percentage of MUC2- and MUC2+ cells in *Bhlha15*$^{+}$Ki67^{+} cells are quantified. Total 150 *Bhlha15*$^{+}$Ki67^{+} cells from 3 mice are analyzed. Mean±S.E.M.

Figure S3. Notch activation in *Bhlha15*-lineage.

(A) (left) TUNEL staining (green) along with RFP (red) and Lysozyme (gray) staining on irradiated *Bhlha15*-CreERT; *R26*-TdTomato mouse intestine. Mice were irradiated at a dose of 10 Gy 1 day after tamoxifen induction, then sacrificed 4 hours later. (right) Cleaved caspase 3 (green) and RFP (red) staining on the same mice. Arrows indicate *Bhlha15*$^{+}$ progenitors. (B) RFP (red) and Lysozyme (green) staining on *Bhlha15*-CreERT; *Lgr5*-DTR-GFP; *R26*-TdTomato mice. Mice were treated with DT 1 day after tamoxifen induction, and sacrificed on the next day. Numbers of TdTomato+ Paneth cells per crypt were quantified. Total 50 crypts per group from 2 mice were counted. (C) HES1 (green) and RFP (red) staining on the small intestines from *Bhlha15*-CreERT; *R26*-TdTomato treated with or without 10 Gy irradiation or doxorubicin, *Bhlha15*-CreERT; *Lgr5*-DTR-GFP; *R26*-TdTomato mice treated with DT, or *Bhlha15*-CreERT; LSL-Notch1(IC); *R26*-TdTomato mice. Arrows indicate double positive cells. Tamoxifen was given at day 0, irradiation, DT, or doxorubicin was given at day 1, and mice were analyzed at day 2. Percentages of HES1^{+} cells in TdTomato^{+} Paneth cells and non-Paneth TA progentors are quantified. Total 300 cells from 3 mice per group are counted. (D) HES1 (green) and RFP (red)

staining on the small intestines from *Bhlha15*-CreERT; *R26*-TdTomato treated with doxorubicin and *Bhlha15*-CreERT; LSL-Notch1(IC); *R26*-TdTomato mice. Mice were analyzed at day 7. (E) *Bhlha15*-CreERT; *R26*-TdTomato and *Bhlha15*-CreERT; LSL-Notch1(IC); *R26*-TdTomato mouse small intestine 30 days after tamoxifen induction. Additional FABP1 staining (green) was added in the right panel. (F-G) Organoids of *Bhlha15*-CreERT; *R26*-mTmG and *Bhlha15*-CreERT; LSL-Notch1(IC); *R26*-mTmG small intestine at day 30 (F). Lysozyme (red) and GFP (green) staining on *Bhlha15*-CreERT; *R26*-mTmG organoids is shown in (G). (H) HES1 (green) and RFP (red) staining on the small intestines from *Bhlha15*-CreERT; *R26*-TdTomato treated with doxorubicin with or without DBZ. Tamoxifen was given at day 0, doxorubicin was given at day 1, DBZ was given daily from day 2 to 4, then mice were analyzed at day 7. Tracing events per 100 crypts in each group were quantified (n=3). Mean±S.E.M. *p<0.05.

Figure S4. Notch activation in *Lgr5* and *Dclk1* lineage.

(A) Lineage tracing images of *Lgr5*-CreERT; *R26*-mTmG mouse small intestine and colon with or without Notch1(IC) expression. Images are taken 2 months after tamoxifen induction. (B) Lineage tracing images of *Dclk1*-CreERT;

LSL-Notch1(IC); *R26*-TdTomato mouse small intestine and colon. Images are taken 14 days after tamoxifen induction. (C) Tracing events per 100 glands with or without Notch1(IC) expresson were quantified (n=3/group). Mean±S.E.M.

Figure S5. Analysis of intestinal *Bhlha15*$^{+}$ and *Lgr5*$^{+}$ cells after injury.

(A) Hierarchical tree clustering of average gene expression in the cells shown in Fig. 5A compared to gene expression in the whole intestine. (B) Numbers of differentially expressed genes (> 2 fold increase or < 0.5 fold decrease, $p < 0.1$) in TdTomato^{+}CD24^{lo} and CD24^{hi} cells after indicated interventions compared to untreated cell populations. (C) GSEA analysis for the comparison between untreated TdTomato^{+}CD24^{lo} and CD24^{hi} cells and cells after *Lgr5*-DT ablation (left) or irradiation (right). (D) (top) *Lgr5*-GFP expression in doxorubucin-treated *Lgr5*-CreERT-IRES-EGFP mice at day 0, 1, and 7. (bottom) Day 7 lineage tracing in *Lgr5*-CreERT-IRES-EGFP; *R26*-TdTomato mice with or without doxorucin. Tamoxifen and doxorubicin were given at day 0. (E) Protocol (left), Ki67 and RFP staining (middle), and quantification of tracing events (right) in *Bhlha15*-CreERT; *Lgr5*-DTR; *R26*-TdTomato mice treated with DT and doxorubicin. (F) GFP+ cell numbers in *Bhlha15*-CreERT; *Lgr5*-DTR-GFP; *R26*-TdTomato mice and *Bhlha15*-CreERT; LSL-Notch1(IC); *Lgr5*-DTR-GFP;

R26-TdTomato mouse intestinal crypts 30 days after tamoxfen. Total 60 crypts per crypts are quantified (n=3). Mean±S.E.M. *p<0.05.

Figure S6. Histology of injured *Bhlha15*-CreERT; *Apc*$^{flox/flox}$ mice, *Bhlha15*-CreERT; *Apc*$^{flox/flox}$; LSL-Notch1(IC) mice, and *Bhlha15*-CreERT; LSL-Notch1(IC); LSL-*Kras*^{G12D}; LSL-*p53*^{R172H} mice.

(A) Day 30 images of *Bhlha15*-CreERT; *Apc*$^{flox/flox}$ mice treated with irradiation or doxorubicin. (B) Low and high power images of day 14 *Bhlha15*-CreERT; *Apc*$^{flox/flox}$; LSL-Notch1(IC) mice. (C) Hes1 (red) and β-catenin (green) staining in *Lgr5*-CreERT; *Apc*$^{flox/flox}$ and *Bhlha15*-CreERT; LSL-Notch1(IC); *Apc*$^{flox/flox}$ mouse small intestine 1 week after tamoxifen. (D) Day 30 images of *Bhlha15*-CreERT; LSL-*Kras*^{G12D}; LSL-*p53*^{R172H} mice and *Bhlha15*-CreERT; LSL-*Kras*^{G12D}; LSL-*p53*^{R172H} ; LSL-Notch1(IC) mice.

Figure S7. *Bhlha15* expression and lineage tracing in the colon.

(A) Cell position of *Bhlha15*$^{+}$ cells in the colon. Cell position is defined as shown in the schema. Total 60 crypts are quantified. (B) In situ hybridyzation of *Bhlha15* and immunohistochemistry of Bhlha15 in the colon. (C) Staining for estrogen receptor (red) in *Bhlha15*-CreERT mouse colon. Negative control image using WT mice is provided. (D) Representative images of *Bhlha15*-CreERT;

Lgr5-DTR-EGFP; *R26*-TdTomato mouse colon 1 day after tamoxifen induction (left), and 5 days after tamoxifen plus DT treatment (right). (E) MUC2, DCLK1, and carbonic anhydrase 2 staining (green) of *Bhlha15*-CreERT; *R26*-TdTomato and *Bhlha15*-CreERT; LSL-Notch1(IC); *R26*-TdTomato mouse colon 5 days after tamoxifen.

Figure S8. DSS activates Wnt/YAP signaling in *Bhlha15*$^{+}$ progenitors in the colon.

(A) Day 30 colon images of *Bhlha15*-CreERT; *R26*-TdTomato mice (control) with or without DSS treatment. (B) Lineage tracing events per swiss-rolled whole colon were quantified in *Bhlha15*-CreERT; *R26*-TdTomato mice (control), *Bhlha15*-CreERT; LSL-Notch1(IC); *R26*-TdTomato mice (NICD), *Bhlha15*-CreERT; *Lgr5*-DTR-EGFP; *R26*-TdTomato mice treated with DT (Lgr5DTR), *Bhlha15*-CreERT; LSL-Notch1(IC); *Lgr5*-DTR-EGFP; *R26*-TdTomato mice treated with DT (NCD+DTR), and *Bhlha15*-CreERT; *R26*-TdTomato mice treated with DSS (DSS) at 30 days after tamoxifen. DT was given 1 day after tamoxifen. 2.5% DSS treatment was started 1 day after tamoxifen and continued for 5 days. n=3/group. (C) FACS plot of *Bhlha15*-CreERT; *Lgr5*-DTR-EGFP; *R26*-TdTomato mouse colon before and

after DSS treatment. Mice were treated or non-treated with 2% DSS for 5 days and given tamoxifen at the last day of DSS. Distal half of the colon was harvested at the next day. Percentage of GFP^+ cells in viable cells is quantified (n=3/group). (D) HES1 (green) and RFP (red) staining on *Bhlha15*-CreERT; *Lgr5*-DTR-EGFP; *R26*-TdTomato mouse colon before and after DSS treatment. Mice were treated or non-treated with 2% DSS for 5 days, given tamoxifen at the last day of DSS, and analyzed at the next day. (E) YAP (green) and RFP (red) staining on *Bhlha15*-CreERT; LSL-Notch1(IC); *R26*-TdTomato and *Bhlha15*-CreERT; *Lgr5*-DTR-EGFP; *R26*-TdTomato mouse colon treated with DT. Tamoxifen and DT were given 1 day prior to sacrifice. (F) Percentages of YAP^+, $pSrc^+$, or cyclin $D1^+$ cells in $TdTomato^+$ cells in the colon shown in Fig. 7D. (G-I) Mice were treated as in Fig. S8A. Gene expression per *B2m* in sorted $TdTomato^+$ cells with or without DSS treatment is shown in (G). n=3/group. β-catenin (green) and RFP (red) staining on *Bhlha15*-CreERT; *R26*-TdTomato mouse colon after DSS treatment is shown in (H). Sorted $TdTomato^+$ cells with or without DSS treatment were cultured as in Fig. 5D, and colony forming efficiency was quantified (n=3/group). (J) Protocol of DSS and Src inhibitor treatment. (K) YAP (green) and RFP (red) staining on DSS-treated *Bhlha15*-CreERT;

R26-TdTomato mouse colon. Vehicle or Src inhibitor was given to the mice (n=3). Numbers of TdTomato^{+} clones containing more than 5 cells per 100 glands were quantified. Mean±S.E.M. *p<0.05.

Figure S9. Comparison of *Apc*-deleted tumors.

(A-C) H&E staining (A), YAP or HES1 (red) and β-catenin (green) staining (B), and gene expression per *B2m* (C) of *Lgr5*-CreERT; *Apc*$^{flox/flox}$ and *Bhlha15*-CreERT; *Apc*$^{flox/flox}$ colon tumors with or without DSS (2%, 5days). *Bhlha15*-CreERT; *Apc*$^{flox/flox}$ colon tumors were harvested at 30 days after tamoxifen, and *Lgr5*-CreERT; *Apc*$^{flox/flox}$ colon tumors were harvested at 20 days after tamoxifen.

Figure S10. Abnormal Notch signaling is associated with CIN-type, left-sided colon cancers with serrated histology in human.

(A) BHLHA15 expression in human small intestine and colon. (B) Oncoprint image obtained from cBioPortal website (http://www.cbioportal.org/). 194 Colorectal cancer cases in TCGA dataset were analyzed. (C) Representative H&E images of serrated-type and non-serrated type colorectal cancers. (D) Overall survival curves of patients with (red) and without (blue) gene alterations in *RBPJL*. (E-F) HES1 staining in human adenomas (E) and ratio of HES1

positivity in different histological polyps (F). (G) Gene expression in *Lgr5*-CreERT; *Apc*$^{flox/flox}$ and *Bhlha15*-CreERT; LSL-Notch1(IC); *Apc*$^{flox/flox}$ small intestine 1 week after tamoxifen.

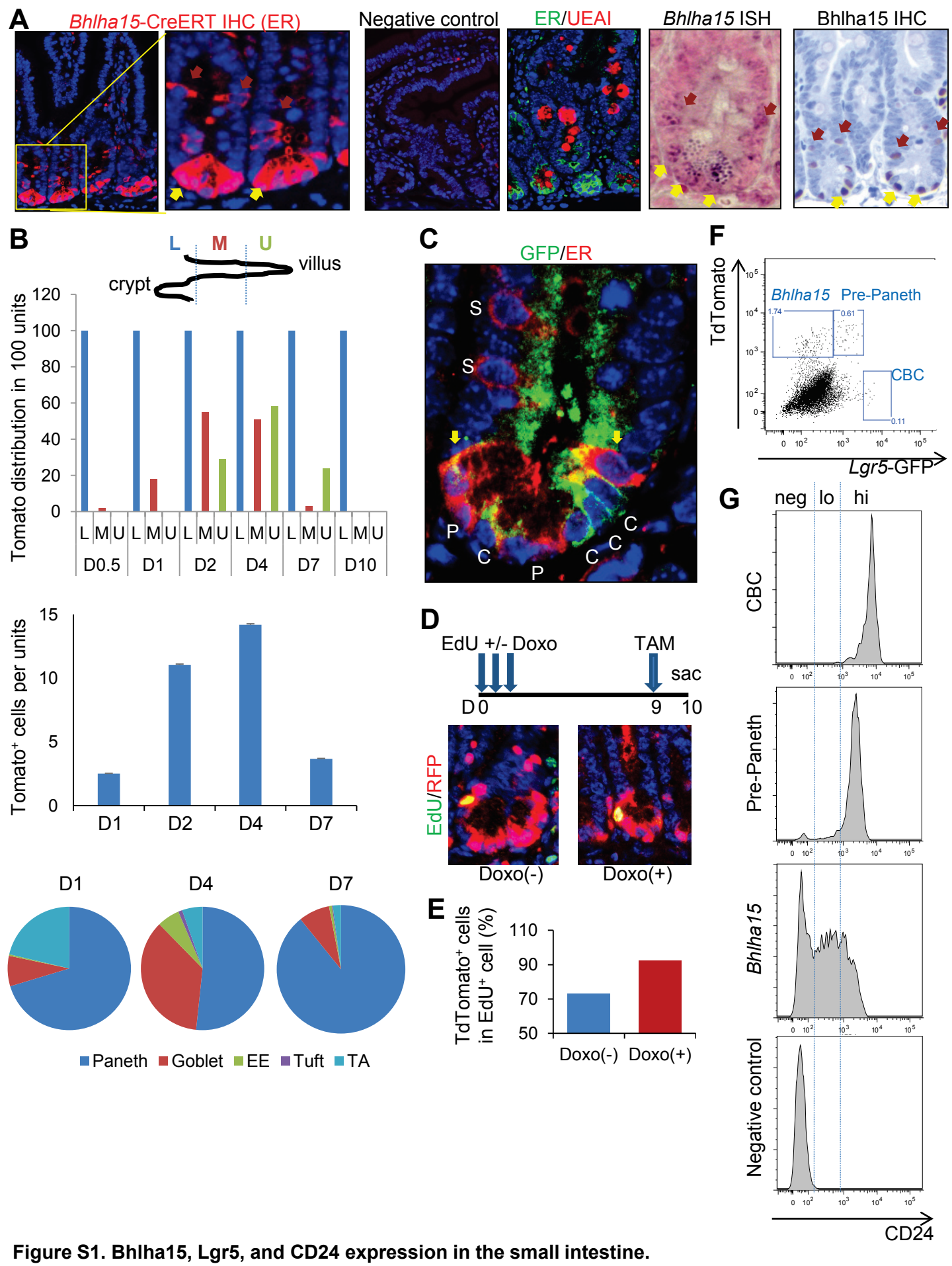

Figure S1. Bhlha15, Lgr5, and CD24 expression in the small intestine.

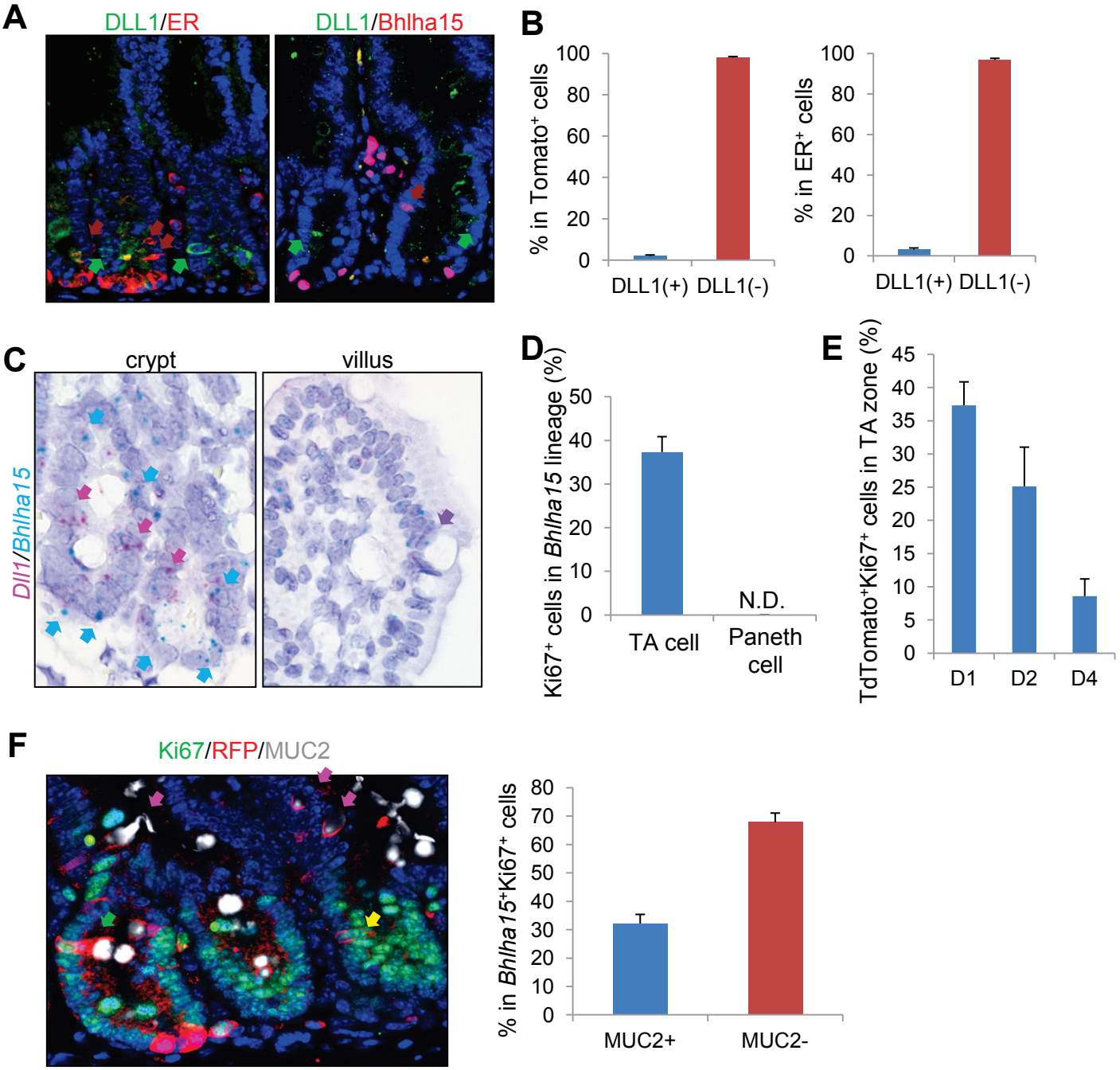

Figure S2. Relationship between Bhlha15 and DLL1 expression in the small intestine.

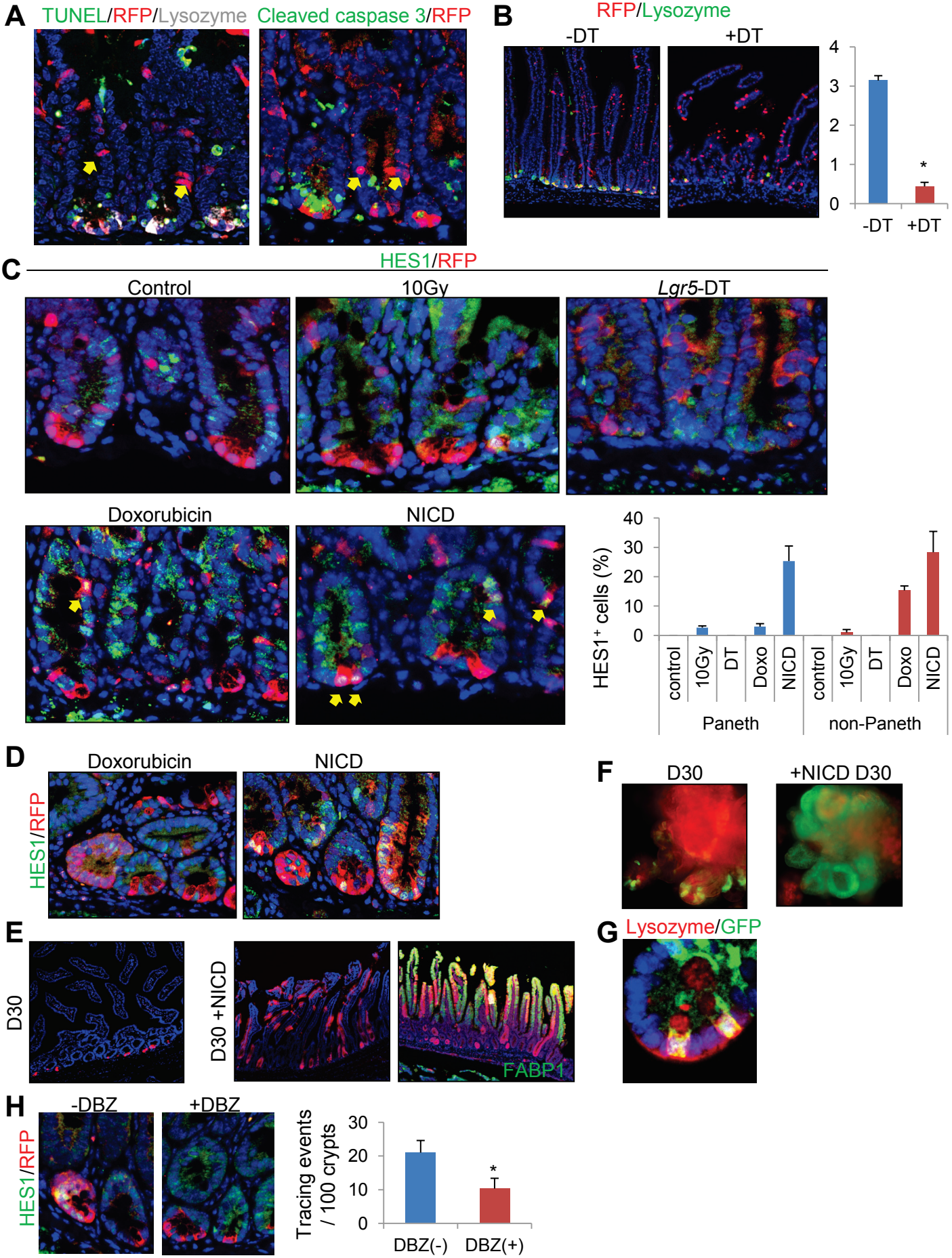

Figure S3. Notch activation in *Bhlha15*-lineage.

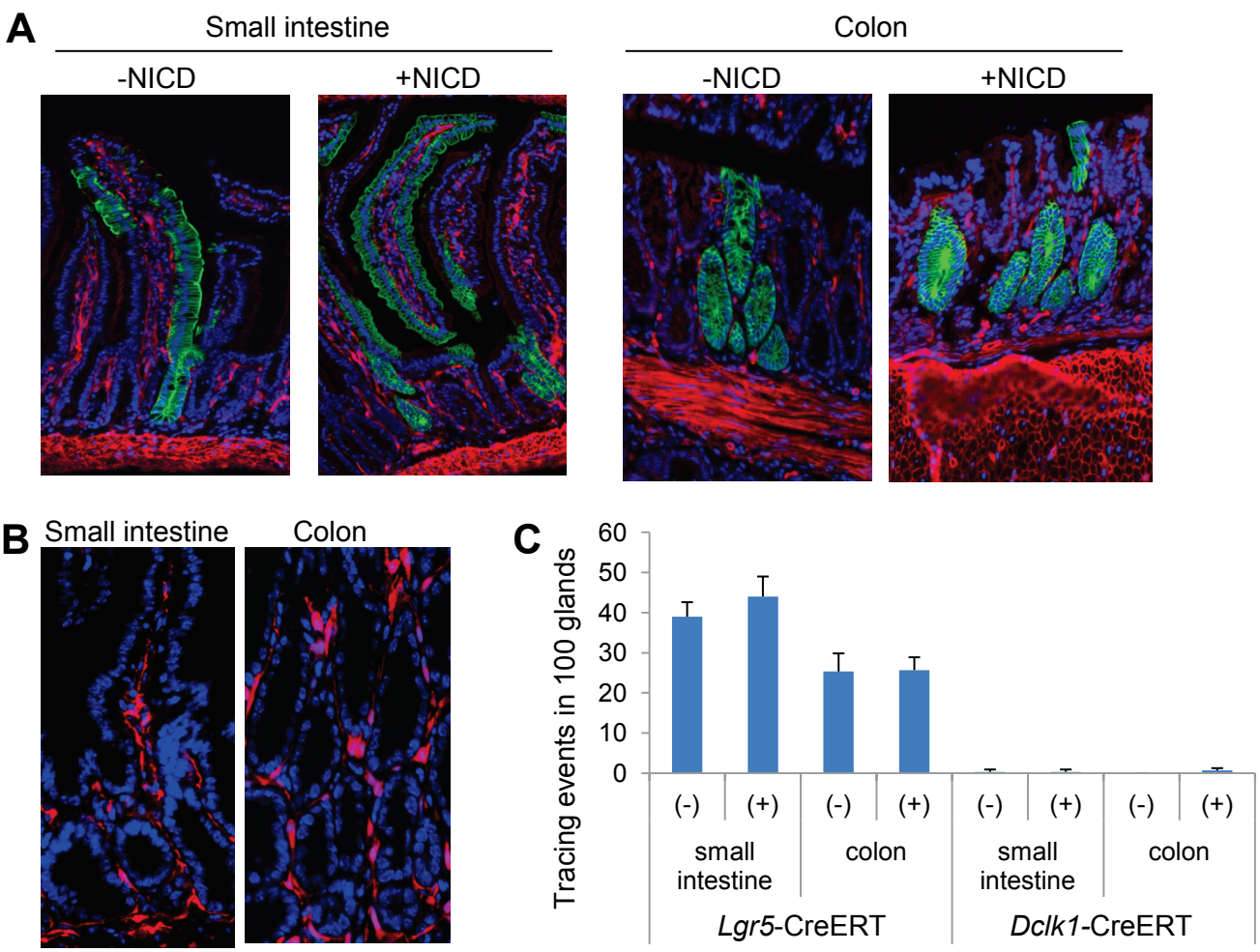

Figure S4. Notch activation in *Lgr5* and *Dclk1* lineage.

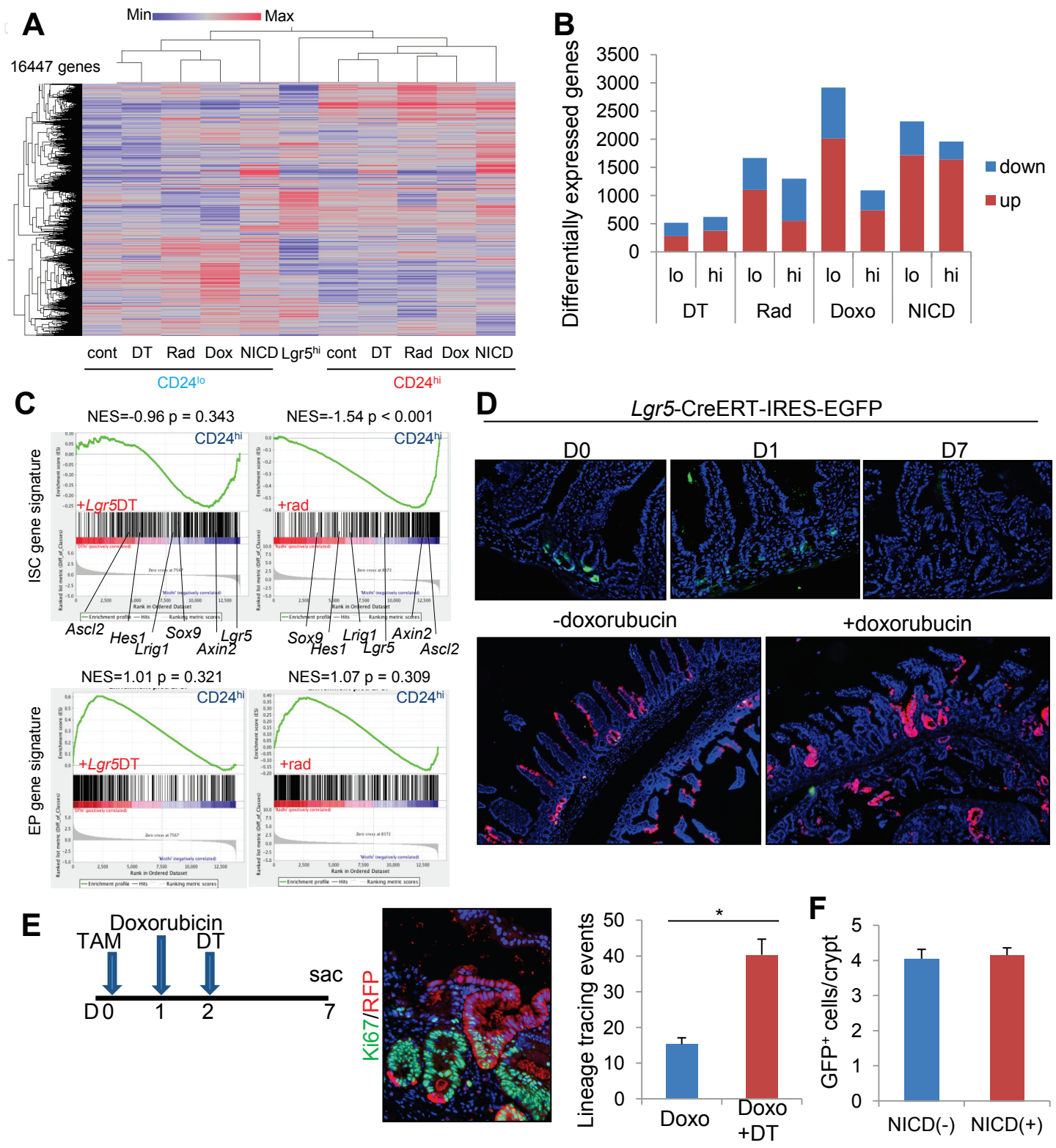

Figure S5. Analysis of intestinal *Bhlha15*⁺ and *Lgr5*⁺ cells after injury.

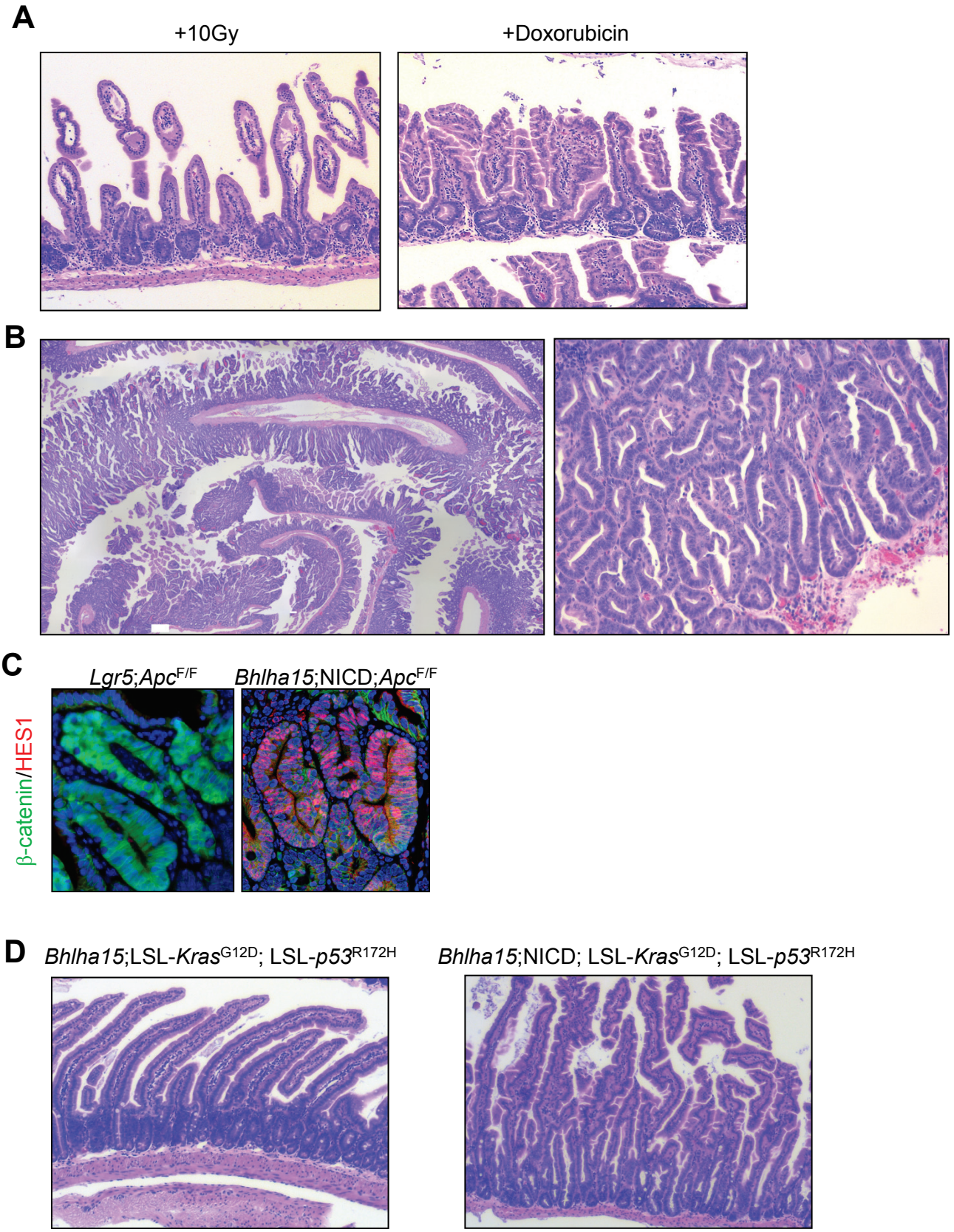

Figure S6. Histology of injured *Bhlha15*-CreERT; *Apc*$^{flox/flox}$ mice, *Bhlha15*-CreERT; *Apc*$^{flox/flox}$; LSL-Notch1(IC) mice, and *Bhlha15*-CreERT; LSL-Notch1(IC); LSL-*Kras*^{G12D}; LSL-*p53*^{R172H} mice.

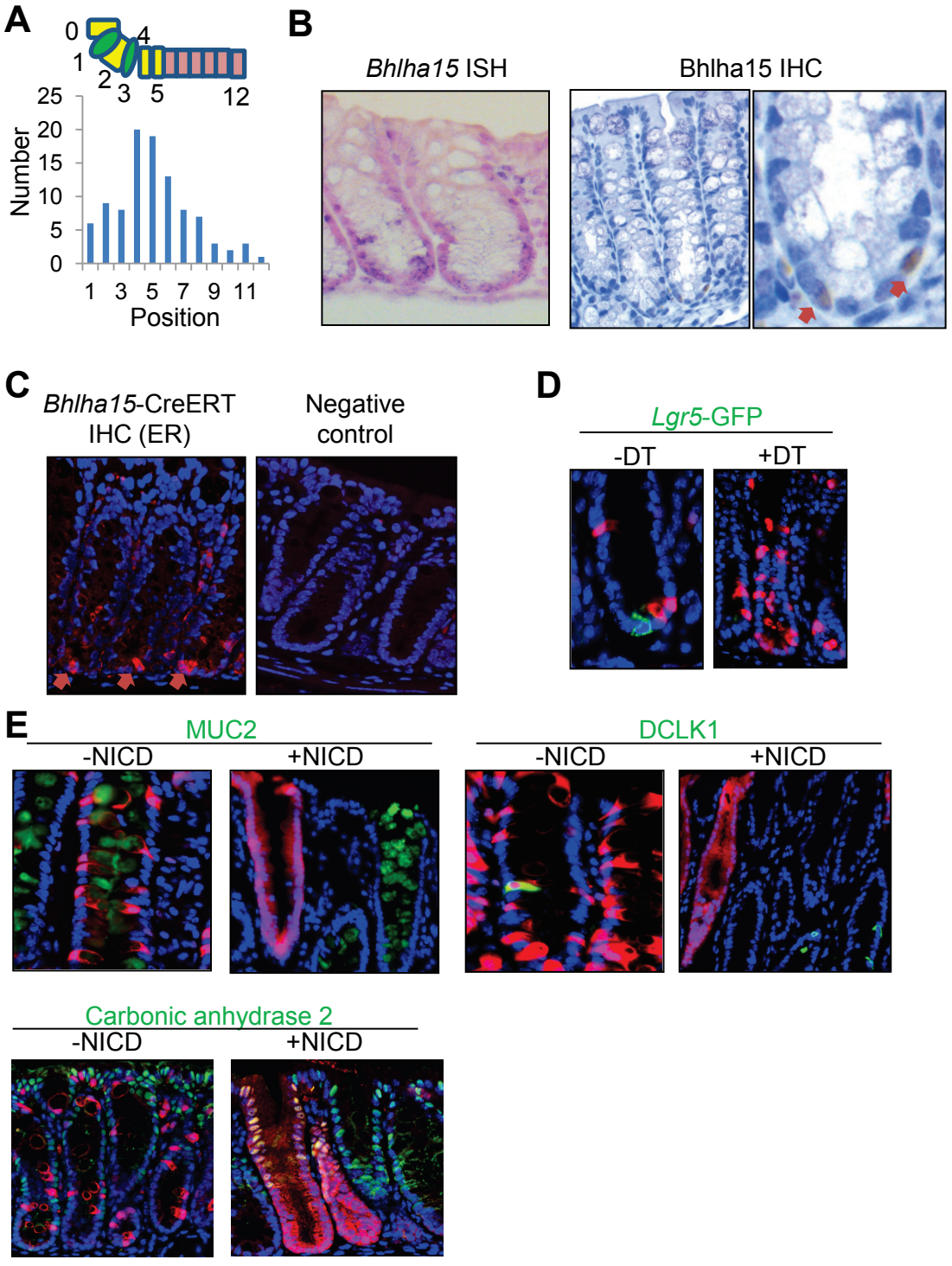

Figure S7. *Bhlha15* expression and lineage tracing in the colon.

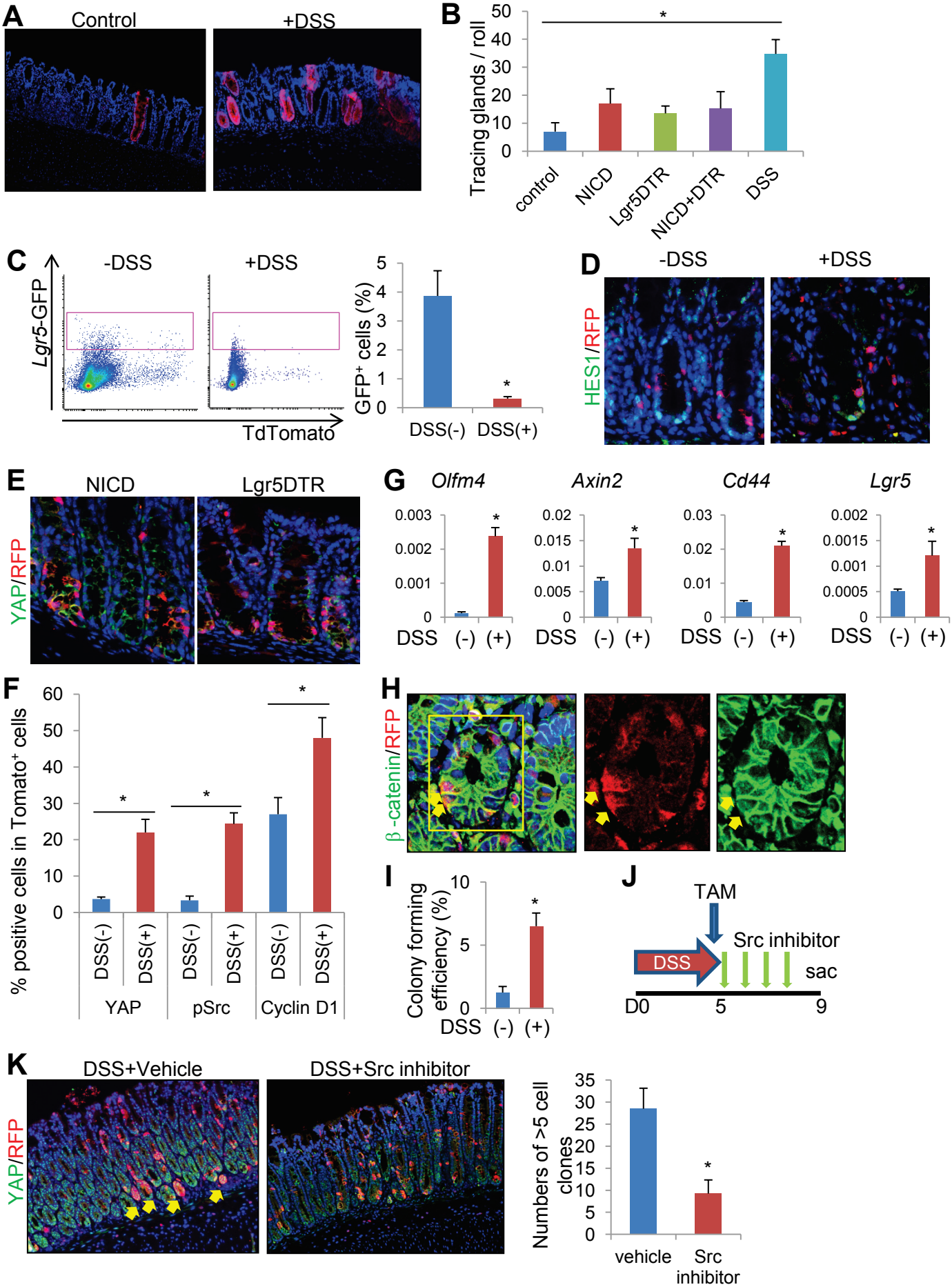

Figure S8. DSS activates Wnt/YAP signaling in *Bhlha15*+ progenitors in the colon.

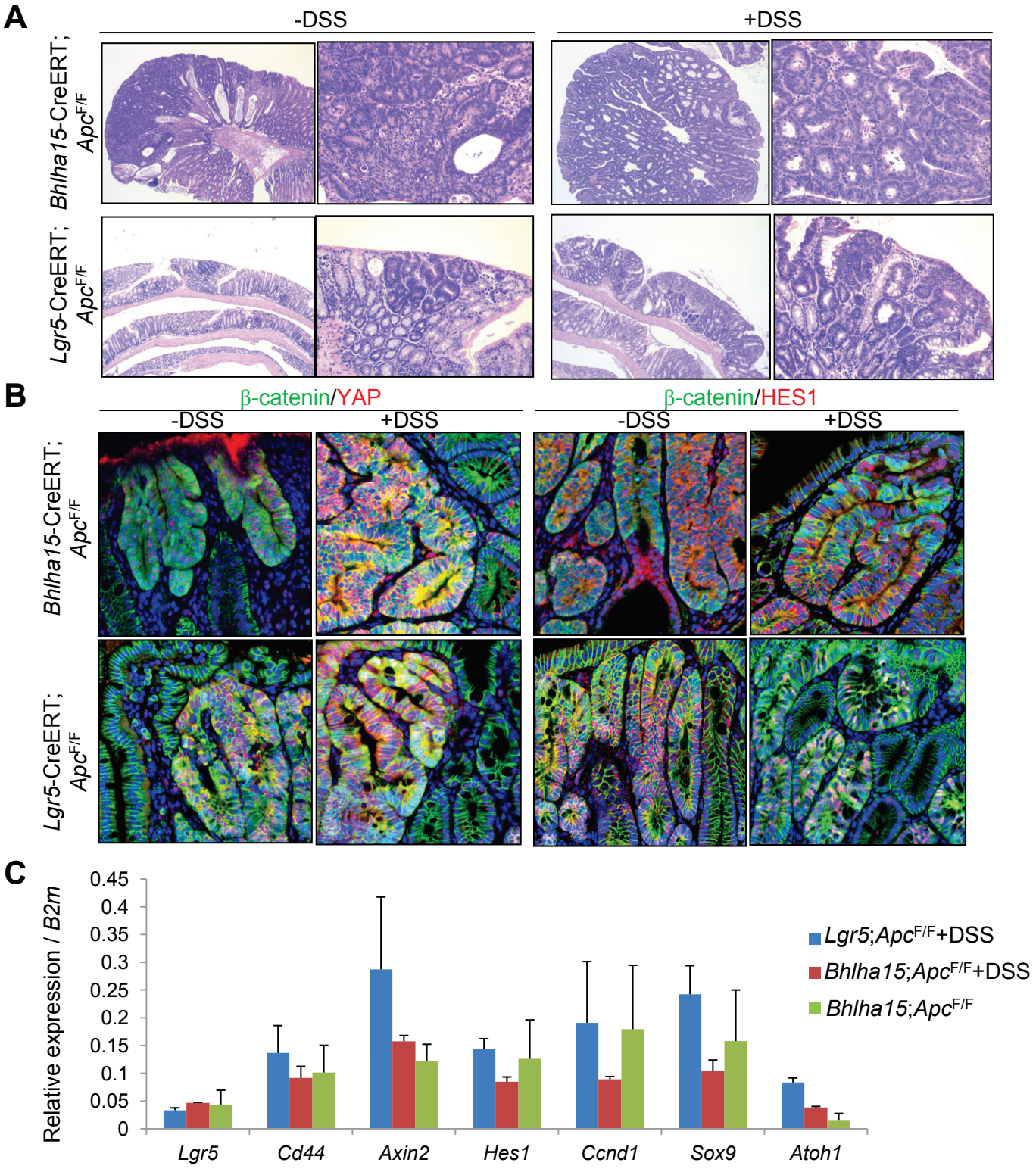

Figure S9. Comparison of *Apc*-deleted tumors.

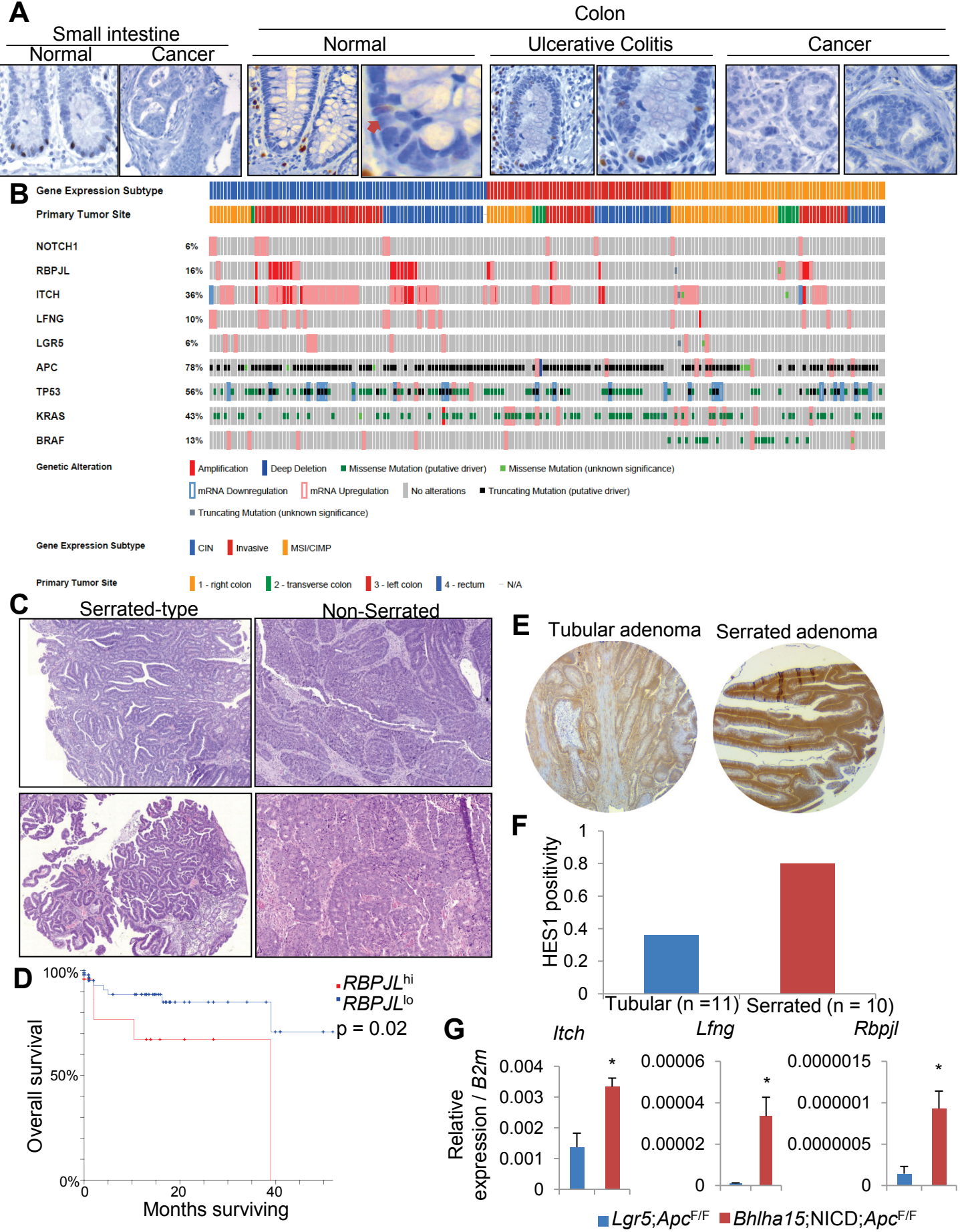

Figure S10. Abnormal Notch signaling is associated with CIN-type, left-sided colon cancers with serrated histology in human.